Support Effect on the Structure and Reactivity of VSbO4 Catalysts for Propane Ammoxidation to Acrylonitrile

4 AUTHORS, INCLUDING:

M. Olga Guerrero-Pérez
University of Malaga
75 PUBLICATIONS **1,072** CITATIONS

SEE PROFILE

Miguel Angel Vicente
Universidad de Salamanca
164 PUBLICATIONS **3,028** CITATIONS

SEE PROFILE

Miguel Banares
Spanish National Research Council
216 PUBLICATIONS **4,439** CITATIONS

SEE PROFILE

Support Effect on the Structure and Reactivity of VSbO₄ Catalysts for Propane Ammoxidation to Acrylonitrile

M. Olga Guerrero-Pérez,*,† J. L. G. Fierro,† Miguel A. Vicente,‡ and Miguel A. Bañares†

Instituto de Catálisis y Petroleoquímica, CSIC, Marie Curie, E-28049-Madrid, Spain, and Departamento de Química Inorgánica, Universidad de Salamanca, Pza. Merced s/n, E-37008-Salamanca, Spain

A new synthesis method for Sb−V−O based catalysts is proposed. VSbO₄ phase is supported both in alumina and in niobia because it is known that such structure is the active phase for acrylonitrile formation. The relevance of the support on the structure and performance of the VSbO₄ phase is evaluated by X-ray diffraction, Raman spectroscopy, and X-ray photoelectron spectroscopy and in the ammoxidation of propane to acrylonitrile. The role of segregated antimony oxide for the VSbO₄ phase is confirmed in VSbO₄/Al₂O₃. In this system, segregated antimony oxide is critical for the redox cycle of vanadium sites. However, a new catalytic phase forms in VSbO₄/Nb₂O₅. Niobia support affords an efficient phase other than VSbO₄ that is selective to acrylonitrile formation. This phase appears to be a Sb-promoted V−Nb−O one.

Introduction

Acrylonitrile production has continuously increased during more than four decades.[1] It is an intermediate widely used for the preparation of synthetic rubbers, synthetic resins, and fibers.[2] It is industrially produced by ammoxidation of propylene, and the direct conversion of propane into acrylonitrile by ammoxidation of propane is an alternative route to the conventional propylene ammoxidation because propane is cheaper than propylene. There are several studies about catalysts used for propane ammoxidation, but the major part of the reported work is concentrated on two types of catalysts, the antimonates with rutile structure[3–7] and the molybdates.[8–12] Most of the formulations for propane ammoxidation are closely related to those of propylene ammoxidation because the reaction appears to occur via propylene.[2,13,14] Thus, the first step in propane ammoxidation is the oxidative dehydrogenation to propylene.[14,15]

Several synthesis methods have been used to prepare the Sb−V−O based catalysts, and it is reported that the synthesis method dramatically affects the behavior of these catalysts.[16] A rather common synthesis method[5] consists in refluxing an aqueous dispersion of NH₄VO₃ or V₂O₅ and Sb₂O₃ during several hours. Others studies try to keep vanadium as V⁴⁺ with oxalic acid and add antimonic acid to such a solution[17] or prepare catalysts with a solution of VCl₃ and SbCl₅ in HCl.[4,18] Sol−gel method synthesis for this kind of catalyst maximizes the Sb−V interaction.[19] Our group has proposed a synthesis method in which Sb is solved with tartaric acid.[20,21]

V−Sb oxides present different segregated phases: V₂O₅, amorphous antimony oxides,[20,21] Sb₂O₃, and α-Sb₂O₄ (β-Sb₂O₄ is only present when calcination temperatures are higher than about 800 °C [16]). Vanadium and antimony can react to form a rutile-like vanadium−antimonate phase (VSbO₄) that is supposed to be the active site, or at least one of the active sites, for acrylonitrile formation.[6,22–27] The interaction between these elements is promoted by calcination

* Corresponding author. E-mail: oguerrero@icp.csic.es. Tel.: +34 91 585 4880. Fax: +34 91 585 4760.
† CSIC.
‡ Universidad de Salamanca.

(1) Grasselli, R. K. *Top. Catal.* **2002,** *21,* 79.
(2) Grasselli, R. K. In *Handbook in Catalysis*; Ertl, G., et al., Eds.; Wiley-VCH: New York, 1997; Vol. V, p 2302.
(3) Centi, G.; Marchi, F.; Perathoner, S. *Appl. Catal., A* **1997,** *149,* 225.
(4) Centi, G.; Mazzoli, P. *Catal. Today* **1996,** *28,* 351.
(5) Guttmann, A. T.; Grasselli, R. K.; Brazdil, J. F.; James, F. 047949 [U.S. Patent 4,788,317], 1988. Guttmann, A. T.; Grasselli, R. K.; Brazdil, J. F.; Suresh, D. D. U.S. Patent 4,788,317, 1988. Guttmann, A. T.; Grasselli, R. K.; Brazdil, J. F. 724226 [U.S. Patent 4746641], 1988. Bartek, J. P.; Guttmann, A.T. U.S. Patent 4,797,381, 1989.
(6) Grasselli, R. K. *Catal. Today* **1999,** *49,* 141.
(7) Guerrero-Pérez, M. O.; Martínez-Huerta, M. V.; Fierro, J. L. G.; Bañares, M. A. *Appl. Catal., A* **2006,** *298,* 1.
(8) Kim, Y. C.; Ueda, W.; Morooka, Y. *Catal. Today* **1992,** *13,* 673.
(9) Ihl, W.; Seob, K. *Stud. Surf. Sci. Catal.* **1995,** *92,* 191.
(10) Kim, J. S.; Woo, S. I. *Appl. Catal., A* **1994,** *110,* 207.
(11) Ushikubo, T.; Oshima, K.; Kayou, A.; Vaarkamp, M.; Hatano, M. *J. Catal.* **1997,** *169,* 394.
(12) Ushikubo, T.; Oshima, K.; Kayou, A.; Hatano, M. *Stud. Surf. Sci. Catal.* **1997,** *112,* 473.
(13) Catani, R.; Centi, G.; Trifirò, F.; Grasselli, R. K. *Ind. Eng. Chem. Res.* **1992,** *31,* 107.
(14) Guerrero-Pérez, M. O.; Peña, M. A.; Fierro, J. L. G.; Bañares, M. A. *Ind. Eng. Chem. Res.* **2006,** *45,* 4537.
(15) Grasselli, R. K.; Burrington, J. D.; Buttrey, D. J.; De Santo, P.; De Santo, P., Jr.; Lugmair, C. G.; Volpe, A. F.; Wingand, T. *Top. Catal.* **2003,** *23,* 5.
(16) Centi, G.; Mazzoli, P.; Perathoner, S. *Appl. Catal., A* **1997,** *165,* 273.
(17) Derouane-Abd Hamid, S. B.; Centi, G.; Pal, P.; Derouane, E. *Top. Catal.* **2001,** *15,* 161.
(18) Centi, G.; Marchi, F. *Stud. Surf. Sci. Catal.* **1996,** *101,* 277.
(19) Brazdil, J. F.; Toft, M. A.; Bartek, J. P.; Teller, R. G.; Cyngier, R. M. *Chem. Mater.* **1998,** *10,* 4100.
(20) Guerrero-Pérez, M. O.; Bañares, M. A. *Catal. Today* **2004,** *96,* 265.
(21) Guerrero-Pérez, M. O.; Fierro, J. L. G.; Bañares, M. A. *Catal. Today* **2006,** *118,* 366.
(22) Teller, R. G.; Antonio, M. R.; Brazdil, J. F.; Grasselli, R. K. *J. Solid State Chem.* **1986,** *67,* 249.
(23) Centi, G.; Perathoner, S. *Appl. Catal., A* **1995,** *124,* 317.
(24) Centi, G.; Perathoner, S.; Trifirò, F. *Appl. Catal., A* **1997,** *157,* 143.
(25) Zanthoff, H. W.; Grünert, W.; Bucholz, S.; Heber, M.; Stievano, L.; Wagner, F. E.; Wolft, G. U. *J. Mol. Catal. A* **2000,** *162,* 443.
(26) Guerrero-Pérez, M. O.; Bañares, M. A. *Chem. Commun.* **2002,** *12,* 1292.

in inert atmosphere and during ammoxidation reaction.[22–27] The formation of $VSbO_4$ after calcination is incomplete; it appears that this phase is further formed during propane ammoxidation by reaction of vanadium and antimony oxides that have not reacted during calcination.[22–28] The formation of $VSbO_4$ during propane ammoxidation reaction has indeed been observed by Raman spectroscopy with *simultaneous* activity measurement (i.e., *operando* study), which shows direct links between the formation of $VSbO_4$ and acrylonitrile yields.[26] The performance of $VSbO_4$ requires segregated α-Sb_2O_4.[2,13,29–31] On the other hand, large amounts of vanadium, especially the V_2O_5 phase, catalyze the oxidation of NH_3 to N_2, lowering the acrylonitrile selectivity.[4] However, dispersed surface vanadium oxide species significantly increase the performance and efficiency of the $VSbO_4$–α-Sb_2O_4 system.[27,32]

Supported $VSbO_4$ catalysts are affected by the specific oxide support and by the total coverage.[33] The dispersion limit of Sb+V on alumina and on niobia is near nine atoms of Sb+V per squared nanometer of oxide support.[27,33] Below such dispersion limit loading, both vanadium and antimony oxides do not combine into $VSbO_4$ when prepared with separate V and Sb precursors. The interaction between alumina and the supported Sb and V sites is difficult[27] because the formation of $AlSbO_4$ requires temperatures above 800 °C[28] whereas $AlVO_4$ is easily detectable by Raman spectroscopy[34,35] and it is not normally detected in alumina supported Sb-V catalysts.[27] However, niobia reacts easily with the supported Sb and V species.[36] This work evaluates catalysts in which a suspension of $VSbO_4$ is deposited on alumina and on niobia at different coverages. Thus, V and Sb are not added separately and it is expected that the intimate V–Sb interation remains maximum. The $VSbO_4$ aggregates would be affected by interaction with the specific oxide support.

Experimental Section

Preparation of Samples. $VSbO_4$ was obtained by drying in a rotatory evaporator at 80 °C an aqueous solution of NH_4VO_3 (Sigma) and antimony;[37] the amounts of precursors for V and Sb were determined to have a nominal Sb/V atomic ratio of 1. The resulting solid was dried at 115 °C for 24 h an then calcined at 660 °C for 12 h and at 750 °C for 24 h. This material was used to impregnate alumina and niobia supports by the slurry method. $VSbO_4$ was kept in suspension under stirring at 80 °C while the support was added. Two supports were used, γ-Al_2O_3 (Girdler Südchemie) and Nb_2O_5 (Niobium Products). This solution was kept under stirring at 80 °C for 50 min, and then it was dried in a rotatory evaporator at 80 °C. The resulting solid was dried at 115 °C for 24 h and then calcined at 400 °C for 4 h. The dispersion limit of Sb+V on alumina or niobia is near nine atoms of Sb+V per squared nanometer of support.[27,33] However, the catalysts were prepared so that the nominal coverage of $VSbO_4$ (Sb+V) would correspond to 50, 100, or 200% its dispersion limit on the corresponding support (i.e., 0.5, 1, and 2 "monolayers").

Characterization. Nitrogen adsorption isotherms (−196 °C) were recorded with an automatic Micromeritics ASAP-2000 apparatus. Prior to the adsorption experiments, samples were outgassed at 140 °C for 2 h. BET areas were computed from the adsorption isotherms (0.05 < P/P_0 < 0.27), taking a value of 0.164 nm^2 for the cross section of the adsorbed N_2 molecule at −196 °C.

The X-ray photoelectron spectroscopy (XPS) spectra were recorded with a VG Escalab 200R electron spectrometer, equipped with a dual Mg/Al anode. The spectra were excited by the nonmonochromatized Mg Kα source (1253.6 eV) operated at 12 kV and 10 mA. The analyzer operated in the constant analyzer energy (CAE) mode. For the individual peak energy regions a pass energy of 20 eV across the hemispheres was used. The sample powders were pressed on copper holders and then mounted on a sample rod place in the pretreatment chamber of the spectrometer. The pressure in the analysis chamber was in the range of 10^{-9} mbar during data collection. The constant charging of the samples was corrected by referencing all the energies to the binding energy of the C 1s peak at 284.9 eV arising from adventitious carbon. The peaks were fitted by a nonlinear least-squares fitting program using a properly weighted sum of Lorentzian and Gaussian component curves after removal of a Shirley-type background. The binding energy values are quoted with a precision of ±0.1 eV.

X-ray diffraction (XRD) patterns were recorded on a Siemens Krystalloflex D-500 diffractometer using Cu Kα radiation (λ = 0.154 18 nm) and a graphite monochromator. The XRD apparatus is calibrated weekly by using an external standard (quartz), and the position of the peaks perfectly matches the JCPDS pattern of this compound. Working conditions were 40 kV, 30 mA, and a scanning rate of 2°/min for Bragg's angles (2Θ) from 5 to 70°. Because of the very small amount of each sample, the diffractograms were registered over glass sample holder specially designed for small samples. The small diameter of this hole makes the X-ray beam also come into contact over a small surface of the glass, giving rise to the typical silica halo, between 20 and 40° 2Θ observed in the diffractogram.

Raman spectra were run with a single monochromator Renishaw System 1000 equipped with a cooled CCD detector (−73 °C) and holographic super-Notch filter. The holographic Notch filter removes the elastic scattering while the Raman signal remains high. The samples were excited with the 514 nm Ar line; the spectral resolution was approximately 3 cm^{-1} and the spectrum acquisition consisted of 20 accumulations of 30 s. The spectra were obtained under dehydrated conditions (ca. 120 °C) in a hot stage (Linkam TS-1500). Hydrated samples were obtained at room temperature after and under exposure to a stream of humid synthetic air.

Activity Measurements. Activity measurements were performed using a conventional microreactor with an online gas chromatograph equipped with flame ionization and thermal conductivity detectors. The correctness of the analytical determinations was checked for each test by verification that the carbon balance (based on the propane converted) was within the cumulative mean error of the

(27) Guerrero-Pérez, M. O.; Fierro, J. L. G.; Vicente, M. A.; Bañares, M. A. *J. Catal.* **2002**, *206*, 339.
(28) Andersson, S. L. T.; Andersson, G.; Centi, G.; Grasselli, R. K.; Sanati, M.; Trifirò, F. *Stud. Surf. Sci. Catal.* **1992**, *75*, 691.
(29) Anderson, S.; Hansen, S.; Wickman, A. *Top. Catal.* **2001**, *15*, 103.
(30) Nilsson, J.; Landa Cánovas, A.; Hanse, S.; Andersson, A. *Catal. Today* **1997**, *33*, 97.
(31) Nilsson, R.; Lindblad, T.; Andersson, A., Song, C.; Hansen, S. *New Developments in Selective Oxidation II*; Elsevier: Amsterdam, 1994; p 293.
(32) Bañares, M. A.; Guerrero-Pérez, M. O.; Fierro, J. L. G.; Cortéz, G. G. *J. Mater. Chem.* **2002**, *12*, 3337.
(33) Guerrero-Pérez, M. O.; Fierro, J. L. G.; Bañares, M. A. *Catal. Today* **2003**, *78*, 387.
(34) Kanervo, J. M.; Harlin, M. E.; Krause, A. O. I.; Bañares, M. A. *Catal. Today* **2003**, *78*, 171.
(35) Khatib, S. J.; Bañares, M. A. *Catal. Today* **2006**, *118*, 353.
(36) Guerrero-Pérez, M. O.; Fierro, J. L. G.; Bañares, M. A. *Phys. Chem. Chem. Phys.* **2003**, *5*, 4032.
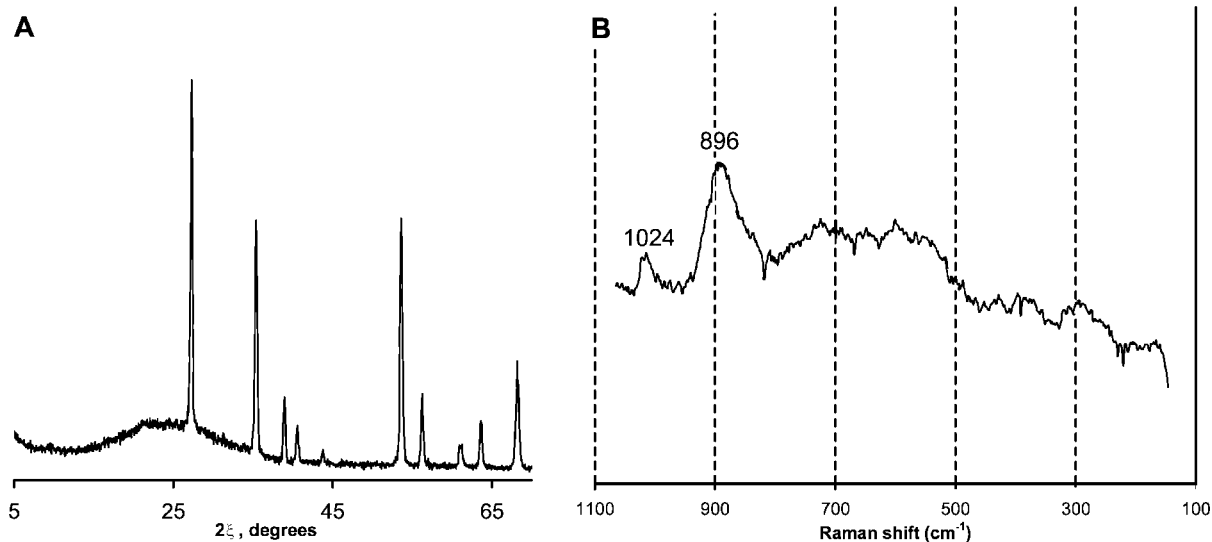(37) Guerrero-Pérez, M. O. Ph.D. Dissertation, Universidad Autónoma de Madrid, Spain, 2003.

Supported VSbO$_4$ Catalysts

Chem. Mater., Vol. 19, No. 26, 2007 6623

Figure 1. XRD pattern (the band between 20 and 40° corresponds to the sampleholder, made in glass) and Raman spectrum of VSbO$_4$ phase.

determinations (±10%). To prevent participation of homogeneous reactivity the reactor was designed to minimize gas-phase activation of propane. Tests were made using 0.2 g of sample with particle dimensions in the 0.25–0.125 mm range. The axial temperature profile was monitored by a thermocouple sliding inside a tube inserted into the catalytic bed. Tests were made using the following feedstock: 25% O$_2$, 9.8% propane, 8.6% ammonia, and helium. The total flow rate was 20 mL/min corresponding to a gas-space velocity (GHSV) of about 3000 h^{-1}. The amount of catalysts and total flow were determined in order to avoid internal and external diffusion contributions.[37] Yields and selectivities in products were determined on the basis of the moles of propane fed and products, considering the number of carbon atoms in each molecule.

Results

Bulk Sb–V–O. The bulk VSbO$_4$ phase was characterized by XRD and Raman spectroscopy (Figure 1). The XRD pattern corresponds to that of VSbO$_4$ (JCPDS files 16-0600 and 30-1412) and to that of VSb$_{1-x}$O$_{4-1.5x}$ phase (JCPDS file 35-1485). The VSbO$_4$ sample exhibits a Raman band centered at 895 cm^{-1} and a weak one near 1020 cm^{-1}, which is partially sensitive to hydration, so it cannot only be assigned to dispersed VOx species. Nilsson et al.[38] have assigned the Raman band near 896 cm^{-1} to the Sb$_{0.92}$V$_{0.92}$O$_4$ phase. Stair et al. reported that this peak around 890 cm^{-1} in VSbOx catalysts arises from Sb vacancies at the surface.[39]

Alumina-Supported Catalysts. The BET area values are shown in Table 1; although similar BET values are obtained for samples with coverages corresponding to 0.5 and 1 monolayers, the lowest value is for the sample with Sb+V coverage above one monolayer. Figure 2A illustrates the diffraction pattern of alumina-supported Sb–V–O catalysts. All the catalysts exhibit diffraction patterns that resemble those of VSbO$_4$ (JCPDS files 16-0600 and 30-1412) and VSb$_{1-x}$O$_{4-1.5x}$ (JCPDS file 35-1485). Both patterns are similar, but a clear shift in the position of the peaks of the supported solids with respect to the JCPDS files is evident.

Table 1. Composition and BET Area of Alumina and Niobia-Supported Sb–V–O Catalysts[a]

support	catalyst	SbVO$_4$ "monolayer"	%SbVO$_4$	BET area m^2/g
Al$_2$O$_3$	0.5VSbO$_4$/Al	0.5	14.2	103
	1VSbO$_4$/Al	1	25.0	106
	2VSbO$_4$/Al	2	40.3	83
Nb$_2$O$_5$	0.5VSbO$_4$/Nb	0.5	13.9	73
	1VSbO$_4$/Nb	1	25.0	58
	2VSbO$_4$/Nb	2	38.2	46

[a] "%SbVO$_4$" means the weight percentage of VSbO$_4$ incorporated in the corresponding support.

Figure 3 illustrates a blow-up in the 26–36° window of the representative pattern of the 1VSbO$_4$/Al catalyst and those of VSbO$_4$ (JCPDS file 16-0600) and of VSb$_{1-x}$O$_{4-1.5x}$ (JCPDS file 35-1485) phases. These shifts are particularly evident for the peaks at 24.5 and 35.2°. Such shifts may be indicative of a distortion in the lattice of the Sb–V–O phase. Comparing the two JCPDS files, for a given reflection peak, the spacing for the VSb$_{1-x}$O$_{4-1.5x}$ phase is slightly higher than for the VSbO$_4$ phase.

The Raman spectra (Figure 2B) of dehydrated alumina-supported Sb–V–O catalysts exhibit several broad bands. All the spectra possess a broadband centered at 800 cm^{-1}, which appears to be constituted by two Raman bands at 835 and 795 cm^{-1} that have been assigned to the VSbO$_4$ phase;[26] these peaks are well-resolved with UV Raman spectroscopy.[39] The spectra present a weak Raman band near 1024 cm^{-1}, sensitive under hydrating conditions, typical of the V=O stretching mode in tetrahedral surface V^{5+} species.[40] Unlike bulk VSbO$_4$, this band is totally affected by hydration, which confirms that it belongs to surface V^{5+} species. The different Raman spectra of bulk and alumina-supported VSbO$_4$ suggest a distortion due to the interaction of the alumina support with the supported Sb–V–O phase that is related with the number of Sb vacancies at the surface.[39] Such interaction alters the structure of the supported phase, as evidenced by the XRD patterns. It appears that part of the V species detaches from the VSbO$_4$ lattice and spreads

(38) Nilsson, R.; Lindblad, T.; Andersson, A. *J. Catal.* **1994**, *148*, 501.
(39) Xiong, G.; Sullivan, V. S.; Stair, P. C.; Zajac, G. W.; Trail, S. S.; Kaduk, J. A.; Golab, J. T.; Brazdil, J. F. *J. Catal.* **2005**, *230*, 317.

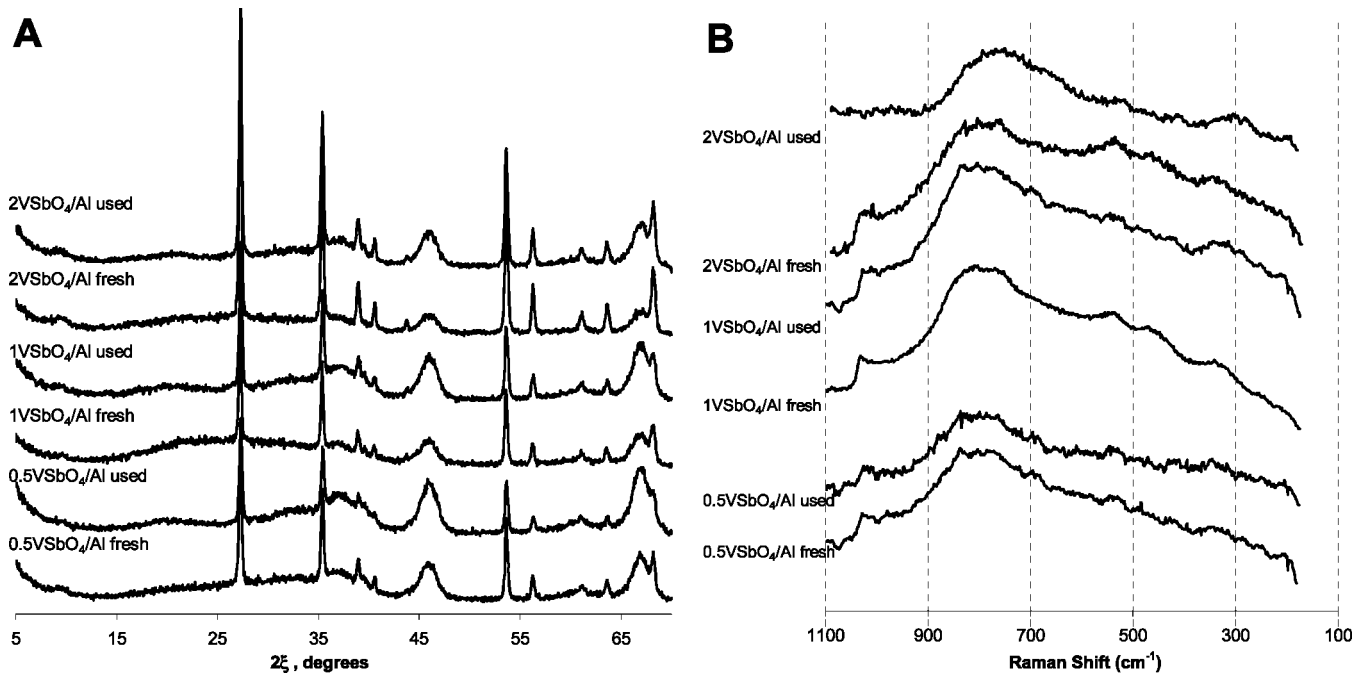(40) Bañares, M. A.; Wachs, I. E. *J. Raman Spectrosc.* **2002**, *33*, 359.

A

B

Figure 2. XRD patterns of fresh and used alumina-supported catalysts (2A) and Raman spectra of fresh and used alumina-supported catalysts (B). The band between 20 and 40° corresponds to the sampleholder, made in glass.
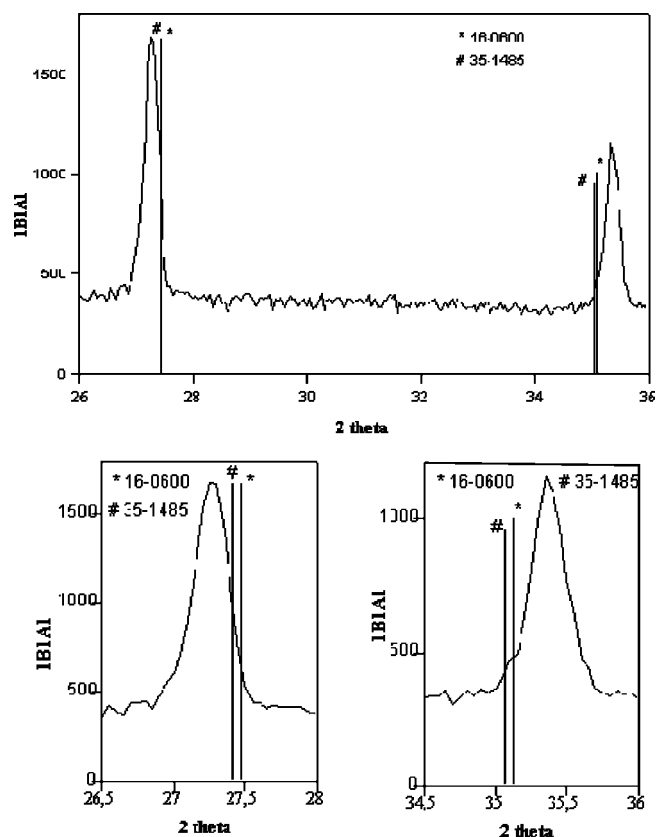

Figure 3. XRD pattern of 1VSbO₄/Al versus JCPDS file 16-0600.

Figure 4. Yields (%) of different products for alumina-supported catalysts and for alumina support. Reaction conditions: total flow 20 mL/min, feed composition (% volume) C₃H₈/O₂/NH₃ (9.8:25:8.6), 200 mg of catalysts, reaction temperature 500 °C.

on the alumina support, possibly as V^{5+} species and creating the Sb vacancies at the surface of VSbO₄ phase. 2VSbO₄/ Al exhibits a different behavior because the fresh catalyst does exhibit the Raman band of surface vanadia species, but this band is absent after use in reaction. In this sample, the total Sb+V loading is twice its dispersion limit loading. Thus, it is likely that the redistribution of V and Sb during reaction
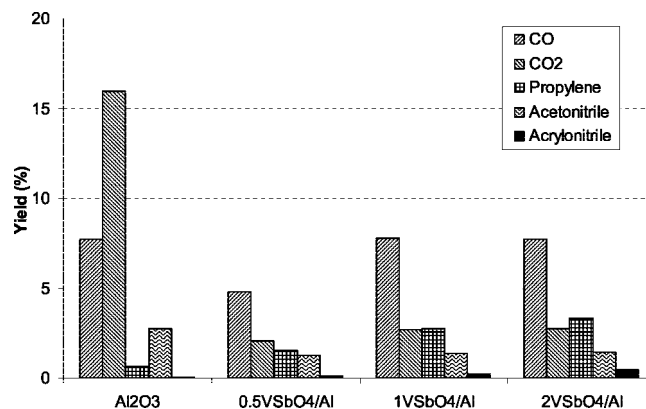
would promote their combination. The tendency of the oxides to spread at lower coverages is due to the availability of support sites. The preference of oxides to spread is due to the more favorable situation of oxides being a dispersed layer rather that a three-dimensional layer on top of the support.[41,42]

Alumina-supported catalysts were stable during time on stream for at least 10 h. Figure 4 shows the yield to the different products at 500 °C for the alumina-supported catalysts, including the alumina support. The addition of the VSbO₄ phase to alumina decreases the total activity of the support, associated to the formation of CO_2. However, VSbO₄ deposited on alumina shows no appreciable activity for propane ammoxidation. COx and propylene are the principal reaction products. The results of this series are worse than

(41) Campbell, C. T. *Surf. Sci. Rep.* **1997**, *27*, 1.
(42) González Elipe, R.; Yubero, F. In *Handbook of Surfaces and Interfaces of Materials*; Nalwa, H.S., Ed.; Academic Press: New York, 2001; Vol. 2, Surface and Interface Analysis and Properties, p 147.

Table 2. Specific Rate of Formation of Acrylonitrile per Vanadium Site at 400 °C

catalyst	(mmol ACN/s)/ mmol V	catalyst	(mmol ACN/s)/ mmol V
0.5VSbO$_4$/Al	0.044	0.5VSbO$_4$/Nb	0.968
1VSbO$_4$/Al	0.050	1VSbO$_4$/Nb	1.625
2VSbO$_4$/Al	0.063	2VSbO$_4$/Nb	3.396

those afforded by Sb−V−O/Al$_2$O$_3$ catalysts prepared by coimpregnation with separate precursors of V and of Sb by the same team, which afford 29% yields to acrylonitrile.[27] Furthermore, the specific rates of acrylonitrile formation per vanadium sites remain very low (Table 2). The difference cannot be related to the composition; it has to lay on the nature of the phases.

Niobia-Supported Catalysts. The BET specific areas of the catalyst are listed in Table 1. The BET area values decrease with Sb+V coverage on Nb$_2$O$_5$. XRD of fresh and used niobia-supported catalysts are shown in Figure 5A. The fresh catalysts present the diffraction patterns of VSbO$_4$ phase (JCPDS file 7-0061), which sharpens for the used samples. Therefore, the niobia support increases its crystallinity during propane ammoxidation reaction.[36]

The Raman spectra of fresh and used niobia-supported dehydrated catalysts are shown in Figure 5B. The Raman spectrum of fresh Nb$_2$O$_5$ support presents Raman bands at 210, 660 and 916 cm^{-1}. The spectrum of the Nb$_2$O$_5$ sample used in propane ammoxidation changes its crystalline phase since the band at 660 shifts to 700 cm^{-1}, the band of 916 cm^{-1} disappear and a weak band appears at 320 cm^{-1}.[36] The better crystallinity of used niobia support evidenced by XRD and Raman spectroscopy is consistent with previous finding in niobia-supported Sb−V−O oxides prepared by coimpregnation with separate V and Sb precursors.[36]

The Raman spectra of used 1VSbO$_4$/Nb and fresh and used 2VSbO$_4$/Nb dehydrated catalysts exhibit a weak broadband near 896 and a weak band near 1020 cm^{-1}, associated to the VSbO$_4$ phase. Because of an increase in the intensity of the Raman bands of niobia support, the weak Raman bands of VSbO$_4$ become hardly visible. The Raman band near 1020 cm^{-1} is sensitive to hydration. Fresh 2VSbO$_4$/Nb exhibits Raman bands of VSbO$_4$, which is poorly Raman scattered, making the appearance of the spectrum noisy (low quality). The crystalline phase changes during reaction, and Nb$_2$O$_5$ Raman bands dominate in the used sample. The Raman bands of Nb$_2$O$_5$ are more intense than those of VSbO$_4$, which accounts for a better signal-to-noise ratio (higher quality).

Niobia-supported catalysts are stable during time on stream for at least 10 h. Figure 6 shows the yields to different reaction products at 500 °C for the VSbO$_4$/Nb series. Propane conversions and selectivities are shown in Table 3. Both propane conversion and acrylonitrile selectivity are higher for niobia-supported samples. Niobia produces essentially propylene and CO$_2$. When VSbO$_4$ is added to niobia the product distribution shifts to acrylonitrile and CO$_2$ formation. At VSbO$_4$ monolayer coverage on niobia and above, the selectivity and yield to acrylonitrile significantly increase. At two monolayers of VSbO$_4$ on niobia, the yield values of acrylonitrile are stable at 23%. Nondesired CO and CO$_2$ form at a much lower extent.

The specific rates for acrylonitrile formation per vanadium site at 500 °C remarkably increase with VSbO$_4$ loading on niobia and are almost 2 orders of magnitude higher than those for the alumina-supported series used here. The nature of the active site must be different to that in the VSbO$_4$/Al series because the product distribution is very different and more selective. The product distribution is also more selective than that of alumina-supported catalysts prepared by coimpregnation of separate V and Sb precursors.[27] The acrylonitrile yields of this series are similar to those afforded by Sb−V−O/Nb$_2$O$_5$ catalysts prepared by coimpregnation with separate precursors of V and Sb by the same team;[36] but in that case higher amounts of other products such as CO$_x$ and propylene were obtained. Niobia sites must interact with VSbO$_4$ phase affording a new active site. XPS should afford additional information about the chemical environments of V and Sb sites on alumina- and niobia-supported series.

XPS Analyses. The energy regions of V 2p, Sb 3d, and O 1s photoelectrons were recorded for representative samples. The energy region of core-level V 2p shows the presence of a strong satellite line coming from the O 1s component because the nonmonochromatic X-ray source was used. Because the principal V 2p$_{3/2}$ component and the O 1s-satellite are separated by approximately 5 eV, the resolution of the V 2p$_{3/2}$ photoelectron is good; however, the less intense V 2p$_{1/2}$ component is overshadowed by this satellite. This is illustrated in Figure 7 where the V 2p + O 1s satellite energy region is presented for the V−Sb−O bulk sample. By applying peak deconvolution procedures, the V 2p$_{3/2}$ peak is satisfactorily described by two components at 516.8 and 515.2 eV, almost of the same intensity (Table 4). These energies can be reasonably ascribed to V^{5+} and V^{3+} species, respectively.[14,43] The observation of these two vanadium species suggests that V^{3+} is the species developed during the synthesis, but some exposed V^{3+} ions oxidize.

Another complication also arises from the Sb 3d doublet. As can be seen in Figure 7, the binding energy of the principal Sb 3d$_{5/2}$ line virtually coincides with that of the O 1s peak. To avoid this uncertainty, we accurately measured the less intense Sb 3d$_{3/2}$ component. For the bulk VSbO$_4$ sample, a value of 540.0 eV was measured for the Sb 3d$_{3/2}$ peak. This value is characteristic of Sb^{5+} species but in no case is associated to Sb^{3+} ions because trivalent antimony species usually display lower energies on the order of 1 eV. For the supported samples on alumina and niobia the same trend is observed. The presence of only Sb^{5+} species, characteristic of bulk VSbO$_4$, is consistent with the absence of segregated Sb oxide phases underlined by XRD and Raman spectra. It can be noted, however, that the V^{5+}/V^{3+} peak area ratios exhibited by the niobia sample is twice that of the alumina counterpart. This difference could be due to the different interactions with the support substrate because V oxide species interact readily with niobia support[44-46]

(43) Anderson, J. A.; Faraldos, M. S.; Weller, S. W.; Bañares, M. A.; Fierro, J. L. G. *J. Catal.* **1997**, *168*, 110.
(44) Smits, R. H. H.; Faraldos, M. S.; Weller, S. W.; Bañares, M. A.; Fierro, J. L. G. *Catal. Today* **1993**, *16*, 513.
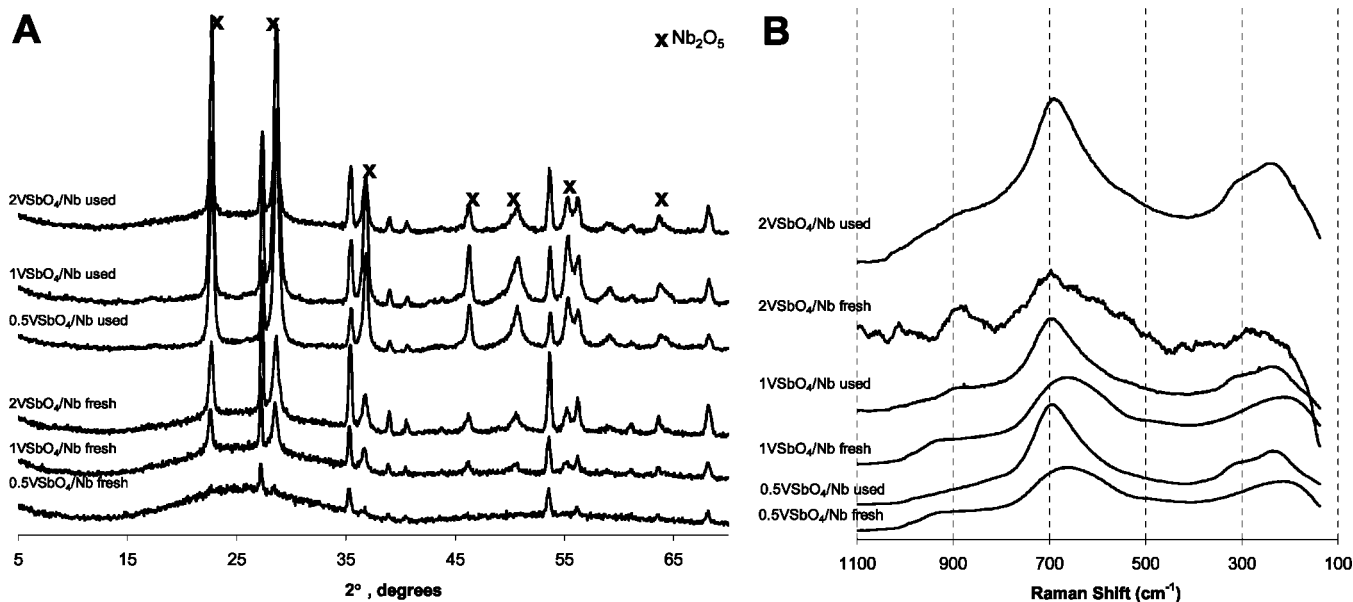
A

B

x Nb$_2$O$_5$

Figure 5. XRD patterns of fresh and used niobia-supported catalysts (A) and Raman spectra of fresh and used niobia-supported catalysts (B). The band between 20 and 40° corresponds to the sampleholder, made in glass.
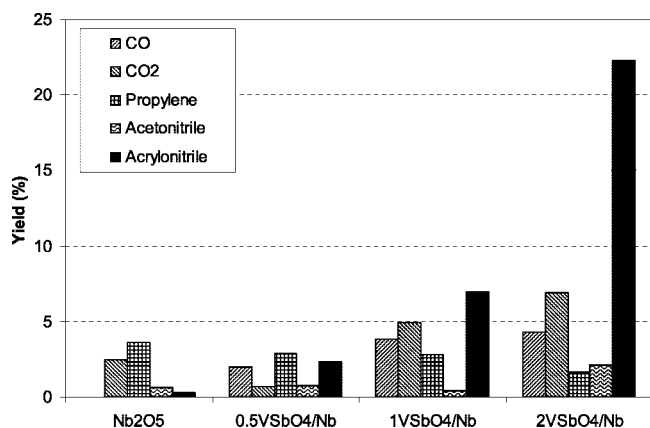

Figure 6. Yields (%) of different products for niobia-supported catalysts and for niobia support. Reaction conditions: total flow 20 mL/min, feed composition (% volume) C$_3$H$_8$/O$_2$/NH$_3$ (9.8:25:8.6), 200 mg of catalysts, reaction temperature, 500 °C.

affording V−Nb−O phases that are efficient for propane ammoxidation.[33] Therefore, the chemical environment of V is different between the niobia-supported and the alumina-supported series. Its higher average oxidation state could be related to its higher activity.

Discussion

About Antimony. The VSbO$_4$ phase is affected by its interaction with the alumina support. These changes can be followed by the 896 cm^{-1} Raman band of bulk VSbO$_4$. Such a band has been reported for bulk Sb−V−O catalysts by the Stair,[39] Wickman,[47] and Nilsson[38] groups. The broad Raman band shifts from 896 cm^{-1} to 820 cm^{-1} when VSbO$_4$

is supported on alumina (Figure 2). This band has also been observed in alumina-supported Sb−V−O catalysts.[27] The XRD pattern shows a distortion of the VSbO$_4$ lattice; thus, it is likely that the shift of the Raman band to 820 cm^{-1} must be due to a component associated to the distortion of VSbO$_4$, that is, to defects. This is in line with the results reported by the Stair's group[39] that associate an increase in the intensity of this Raman band with an increase in the number of Sb vacancies. The catalytic performance of the present alumina-supported catalysts is very poor, as compared with previous V−Sb−O/Al$_2$O$_3$ series prepared by the same team by coimpregnation with separate V and Sb precursors.[27] There is an important difference with such alumina-supported series: XPS, XRD, and Raman spectroscopy show that there is no segregated Sb oxide phase.[27] Segregated Sb oxides show no activity for propane ammoxidation,[27,33] but they couple with VSbO$_4$ into an efficient catalytic system for propane ammoxidation.[2,13,14,26,27,32] It has been proposed that a segregated antimony phase participates in the redox cycle on vanadium species in VSbO$_4$.[2,20,26] The dynamic states of V and Sb appear to be more flexible if segregated Sb oxide species are present along with VSbO$_4$ phases.[2,26,48] Our XPS results agree with previous literature on the oxidation states in VSbO$_4$, V^{3+} and Sb^{5+}.[49,50] Operando Raman−GC studies provide experimental evidence of the dynamic character of VSbO$_4$ interacting with dispersed vanadium oxide species and with segregated Sb oxides.[26,20,51] The redox cycle of vanadia species between surface V^{5+} and V^{3+} in VSbO$_4$ appears facilitated by the presence of segregated Sb$_2$O$_3$ that hosts migrating Sb^{5+} species from VSbO$_4$, forming α-Sb$_2$O$_4$ (mixed-valence oxide) to compensate for V^{3+} species that leave the VSbO$_4$ lattice as a result of their oxidation toward

(45) Simts, R. H. H.; Seshan, K.; Ross, J. R. H.; van der Oetelaar, L. C. A.; Hlewegen, H. J. H. M.; Anantharaman, M. R.; Brongersma, H. H. *J. Catal.* **1995**, *157*, 584.
(46) Ziolek, M. *Catal. Today* **2003**, *78*, 47.
(47) Wickman, A.; Wallenberg, L. R.; Anderson, A. *J. Catal.* **2000**, *194*, 153.
(48) Bychkov, V. Y.; Sivev, M. Y.; Vislovskii, V. P. *Kinet. Catal.* **2001**, *42*, 574.
(49) Berry, F. J.; Brett, M. *Inorg. Chim. Acta* **1983**, *76*, L205.
(50) Birchall, T.; Sleight, A. E. *Inorg. Chem.* **1976**, *15*, 868.
(51) Guerrero-Pérez, M. O.; Bañares, M. A. *J. Phys. Chem. C* **2007**, *111*, 1315.

Supported VSbO₄ Catalysts

Chem. Mater., Vol. 19, No. 26, 2007 6627

Table 3. Propane Conversions and Selectivities of Principal Reaction Products[a]

	conversion (%)			selectivity (%)			
	C_3H_8	CO	CO_2	propylene	acetonitrile	acrylonitrile	acrolein
0.5SbVO₄/Al	9.8	49.1	21.1	15.9	12.6	1.1	0.2
1SbVO₄/Al	14.8	52.5	18.2	18.5	9.2	1.4	0.1
2SbVO₄/Al	15.7	49.3	17.5	21.0	9.3	2.8	0.1
0.5SbVO₄/Nb	8.6	23.1	7.7	33.7	8.6	26.8	0.0
1SbVO₄/Nb	18.9	20.1	26.1	14.9	2.1	36.9	0.0
2SbVO₄/Nb	37.2	11.6	18.5	4.4	5.6	59.7	0.0

[a] Reaction conditions: total flow 20 mL/min, feed composition (% volume) $C_3H_8/O_2/NH_3$ (9.8:25:8.6), 200 mg of catalysts, reaction temperature 500 °C.
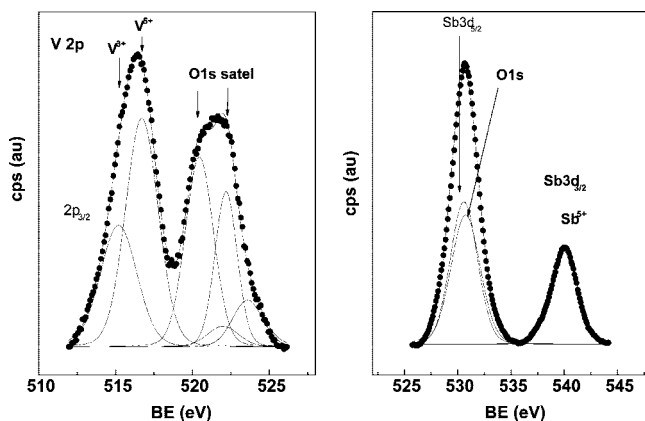

Figure 7. Energy region of V 2p and O 1s (left panel) and of Sb 3d and O 1s (right panel) for bulk the VSbO₄ sample.

Table 4. Binding Energies (eV) of Core Electrons of Sb−V−O Samples[a]

sample	V $2p_{3/2}$	Sb $3d_{3/2}$	Al 2p	Nb $3d_{5/2}$
VSbO₄ bulk	516.8 (49)	540.0		
	515.2 (51)			
1VSbO₄/Al	516.9 (39)	539.8	74.5	
	515.2 (61)			
1VSbO₄/Nb	516.8 (77)	540.1	540.1	207.4
	515.3 (23)			

[a] Values in parentheses indicate the peak percentage.

surface V^{5+} species.[26] Such migration is reversible upon reduction of surface V^{5+} to V^{3+} into VSbO₄. The structural cycle of antimony to accommodate the redox cycle of vanadium is not possible in the absence of segregated antimony oxide. XPS, XRD, and Raman characterization shown that the present preparation method affords no segregated Sb oxide necessary for the catalytic cycles. Thus, the lack of activity for propane ammoxidation in the present series of alumina-supported VSbO₄ catalysts (Figure 4) confirms the relevance of segregated Sb oxide.

About Vanadium. The surface vanadium oxide species appear to be critical for propane activation.[24,28] The V=O group has been proposed as the active site for alkane activation during ammoxidation reaction;[2,13-15] however, the exact nature of the functionality that accounts for alkane activation is still under debate. The first step in ammoxidation reaction is the dehydrogenation of propane to propylene.[2,13,14] For alkane oxidative dehydrogenation, it has been shown that the terminal V=O bond must be ruled out for oxidative dehydrogenation reactions[40,52] of ethane,[53,54] propane,[55,56]

and butane.[57,58] Thus, the active functionality must be bridging oxygen connected to surface vanadium sites. *Operando* Raman−GC studies illustrate that the presence of surface vanadia species proves critical to significantly increase total yield values to acrylonitrile and the specific rate of acrylonitrile formation per vanadium site.[32] Alumina-supported series present VOx surface species, evidenced by the 1030 cm⁻¹ Raman band, but no segregated antimony appears to be present (Figure 2B). Available oxidized vanadium sites are more efficient for alkane activation. For the alumina-supported VSbO₄ system, the presence of surface vanadium oxide species (V^{5+}) accounts for higher conversion of propane to acrylonitrile.[32] Thus, the higher average oxidation state of vanadium in the niobia series may contribute to its higher performance. The nature of the active phase must be different because the product distribution is very different and more selective than that of the Sb−V−O/Al₂O₃ series.

About Niobia. The niobia-supported Sb−V−O catalysts prepared with vanadium and antimony precursors presented a Raman band near 845 cm⁻¹, assigned to the SbNbO₄ phase.[36] Nb may combine with V or with Sb. Mixed Sb-Nb oxides are not active for propane activation.[36] The niobia-supported catalysts series present the VSbO₄ phase, unlike the niobia-supported catalysts prepared by the same team by coimpregnation of separate Sb and V precursors.[36] In that case, "vertical" interactions between niobia support and the supported oxides dominate, at the expense of the V−Sb interaction. The present niobia-supported series exhibits VSbO₄ phase but no segregated α-Sb₂O₄. Thus, the VSbO₄ system should not be active for propane ammoxidation, which is consistent with prior knowledge.[2,59] However, niobia-supported Sb−V−O affords high yield values to acrylonitrile with high selectivity. A possible site isolation of the active sites in VSbO₄ appears unlikely in this case; because the V−Nb−O system is active for propane ammoxidation in the absence of antimony,[33] thus Sb must be a promoter in this system. This is consistent with the finding that the performance of the Nb−Sb−V−O system must be due to a phase other than VSbO₄.[33,36] This new phase affords a different product distribution that makes it more selective.[33,36]

(52) Bañares, M. A. *Catal. Today* **1999**, *51*, 319.
(53) Bañares, M. A.; Martínez-Huerta, M. V.; Gao, X.; Wachs, I. E.; Fierro, J. L. G. *Stud. Surf. Sci. Catal.* **2000**, *130A*, 3125.
(54) Bañares, M. A.; Gao, X.; Fierro, J. L. G.; Wachs, I. E. *Stud. Surf. Sci. Catal.* **1997**, *107*, 295.
(55) Garcia Cortez, G.; Bañares, M. A. *J. Catal.* **2002**, *209*, 197.
(56) Garcia Cortez, G.; Fierro, J. L. G.; Bañares, M. A. *Catal. Today* **2003**, *78*, 219.
(57) Wachs, I. E.; Jehng, J. M.; Deo, G.; Weckhuysen, B. M.; Guliants, V. V.; Benziger, J. B.; Sundaresan, S. *J. Catal.* **1997**, *170*, 75.
(58) Wachs, I. E.; Jehng, J. M.; Deo, G.; Weckhuysen, B. M.; Guliants, V. V.; Benziger, J. B. *Catal. Today* **1996**, *32*, 47.
(59) Grasselli, R. K. *Top. Catal.* **2001**, *15*, 93.

The exact nature of this new phase is not clear yet. Several scenarios may account for the different performances of the Nb-containing catalysts, considering the possible combinations of Sb, V, and Nb species. SbNbO$_4$ is inert while V-Nb-O and V−Sb-O phases are efficient for propane ammoxidation.[33,36] The presence of Sb promotes the performance of V−Nb−O phases as long as it does not coordinate with Nb.[36] The intense Raman bands of niobia support make difficult the determination of the exact nature of the active phase in the Nb−Sb−V−O system, but XPS data suggest that the average oxidation state of vanadium is higher than in the Sb−V−O/Al$_2$O$_3$ system (Table 3). The Nb−Sb−V−O catalysts prepared here and those prepared from separate Sb and V precursors[36] afford similar activity values. The nature of the active site is not clear at this moment: Nb may promote the performance of the VSbO$_4$ phase or it may integrate in the VSbO$_4$ phase. In the latter case, it is likely that the strong Sb−Nb affinity would lead to a deactivation of the system due to the formation of inert NbSbO$_4$ at the expense of the efficient Sb−V−O and Nb−V−O phases.[36] The large increase in the V^{5+}/V^{3+} ratio for the niobia-supported catalyst (Table 3) is indicative of some V−Nb interaction. Thus, the new active phase must involve some interaction between Nb sites and VSbO$_4$ phases affording a new phase with a better catalytic performance.

Conclusions

Alumina-supported VSbO$_4$ distorts by interaction with alumina. This phase does depend on segregated antimony oxide to operate efficiently during propane ammoxidation. The redox cycle of the vanadia sites appears facilitated by the segregated α-Sb$_2$O$_4$ phase.

The high affinity of niobia for antimony and for vanadia renders a catalytic system different to VSbO$_4$. The performance of the Nb−Sb−V−O system is more selective than that of Sb−V−O phases. Such a new active phase appears to be a Nb−V−O phase where the average oxidation state of vanadium is higher than in the VSbO$_4$ system. Sb may promote this system, but it should not coordinate to Nb. Vanadium sites must account for the propane activation in both systems; the different nature of the catalytic phases is consistent with the different product distribution. The Nb-containing system is more selective and active for propane ammoxidation to acrylonitrile than the V−Sb−O.

CM702022D